Generation of quasi-monoenergetic electron beams with small normalized divergences angle from a 2 TW laser facility

D. Z. Li,[1,2] W. C. Yan,[2] L. M. Chen,[2,*] K. Huang,[2] Y. Ma,[2] J. R. Zhao,[2] L. Zhang,[2] N. Hafz,[3] W. M. Wang,[2] J. L. Ma,[2] Y. T. Li,[2] Z. Y. Wei,[2] J. Gao,[1] Z. M. Sheng,[3] and J. Zhang[3]

[1]*Institute of High Energy Physics, CAS, Beijing 100049, China*
[2]*Beijing National Laboratory of Condensed Matter Physics, Institute of Physics, CAS, Beijing, 100190, China*
[3]*Department of Physics and Key Laboratory for Laser plasma (Ministry of Education) Shanghai Jiao Tong University, Shanghai 200240, China*
[*]*lmchen@iphy.ac.cn*

Abstract: We report the generation of a 6 pC, 23 MeV electron bunch with the energy spread ± 3.5% by using 2 TW, 80 fs high contrast laser pulses interacting with helium gas targets. Within the optimized experimental condition, we obtained quasi-monoenergetic electron beam with an ultra-small normalized divergence angle of 92 mrad, which is at least 5 times smaller than the previous LPA-produced bunches. We suggest the significant decrease of the normalized divergence angles is due to smooth transfer from SM-LWFA to LWFA. Since the beam size in LPA is typically small, this observation may explore a simple way to generate ultralow normalized emittance electron bunches by using small-power but high-repetition-rate laser facilities.

OCIS codes: (020.2649) Strong field laser physics; (350.4990) Particles; (350.5400) Plasmas.

References and links

1. T. Tajima and J. M. Dawson, "Laser electron acceleration," Phys. Rev. Lett. **43**(4), 267–270 (1979).
2. S. P. Mangles, C. D. Murphy, Z. Najmudin, A. G. R. Thomas, J. L. Collier, A. E. Dangor, E. J. Divall, P. S. Foster, J. G. Gallacher, C. J. Hooker, D. A. Jaroszynski, A. J. Langley, W. B. Mori, P. A. Norreys, F. S. Tsung, R. Viskup, B. R. Walton, and K. Krushelnick, "Monoenergetic beams of relativistic electrons from intense laser-plasma interactions," Nature **431**(7008), 535–538 (2004).
3. C. G. R. Geddes, C. S. Toth, J. Van Tilborg, E. Esarey, C. B. Schroeder, D. Bruhwiler, C. Nieter, J. Cary, and W. P. Leemans, "High-quality electron beams from a laser wakefield accelerator using plasma-channel guiding," Nature **431**(7008), 538–541 (2004).
4. J. Faure, Y. Glinec, A. Pukhov, S. Kiselev, S. Gordienko, E. Lefebvre, J. P. Rousseau, F. Burgy, and V. Malka, "A laser-plasma accelerator producing monoenergetic electron beams," Nature **431**(7008), 541–544 (2004).
5. W. P. Leemans, B. Nagler, A. J. Gonsalves, C. Tóth, K. Nakamura, C. G. R. Geddes, E. Esarey, C. B. Schroeder, and S. M. Hooker, "GeV electron beams from a centimetre-scale accelerator," Nat. Phys. **2**(10), 696–699 (2006).
6. H. Y. Lu, M. Liu, W. Wang, C. Wang, J. Liu, A. Deng, J. Xu, C. Xia, W. Li, H. Zhang, X. Lu, C. Wang, J. Wang, X. Liang, Y. Leng, B. Shen, K. Nakajima, R. Li, and Z. Xu, "Laser wakefield acceleration of electron beams beyond 1 GeV from an ablative capillary discharge waveguide," Appl. Phys. Lett. **99**(9), 091502 (2011).
7. S. Kneip, S. R. Nagel, S. F. Martins, S. P. D. Mangles, C. Bellei, O. Chekhlov, R. J. Clarke, N. Delerue, E. J. Divall, G. Doucas, K. Ertel, F. Fiuza, R. Fonseca, P. Foster, S. J. Hawkes, C. J. Hooker, K. Krushelnick, W. B. Mori, C. A. J. Palmer, K. T. Phuoc, P. P. Rajeev, J. Schreiber, M. J. V. Streeter, D. Urner, J. Vieira, L. O. Silva, and Z. Najmudin, "Near-GeV acceleration of electrons by a nonlinear plasma wave driven by a self-guided laser pulse," Phys. Rev. Lett. **103**(3), 035002 (2009).
8. X. M. Wang, R. Zgadzaj, N. Fazel, Z. Y. Li, S. A. Yi, X. Zhang, W. Henderson, Y. Y. Chang, R. Korzekwa, H. E. Tsai, C. H. Pai, H. Quevedo, G. Dyer, E. Gaul, M. Martinez, A. C. Bernstein, T. Borger, M. Spinks, M. Donovan, V. Khudik, G. Shvets, T. Ditmire, and M. C. Downer, "Quasi-monoenergetic laser-plasma acceleration of electrons to 2 GeV," Nat Commun **4**, 1988 (2013).
9. H. T. Kim, K. H. Pae, H. J. Cha, I. J. Kim, T. J. Yu, J. H. Sung, S. K. Lee, T. M. Jeong, and J. Lee, "Enhancement of electron energy to the multi-GeV regime by a dual-stage laser-wakefield accelerator pumped by petawatt laser pulses," Phys. Rev. Lett. **111**(16), 165002 (2013).
10. A. Pukhov and J. Meyer-ter Vehn, "Laser wake field acceleration: the highly non-linear broken-wave regime," Appl. Phys. B **74**(4-5), 355–361 (2002).

#206679 - $15.00 USD Received 20 Feb 2014; revised 7 Apr 2014; accepted 14 Apr 2014; published 20 May 2014

11. W. Lu, C. Huang, M. Zhou, W. B. Mori, and T. Katsouleas, "Nonlinear theory for relativistic plasma wakefields in the blowout regime," Phys. Rev. Lett. **96**(16), 165002 (2006).
12. E. Esarey, C. B. Schroeder, and W. P. Leemans, "Physics of laser-driven plasma-based electron accelerators," Rev. Mod. Phys. **81**(3), 1229–1285 (2009).
13. V. Malka, S. Fritzler, E. Lefebvre, M. M. Aleonard, F. Burgy, J. P. Chambaret, J. F. Chemin, K. Krushelnick, G. Malka, S. P. D. Mangles, Z. Najmudin, M. Pittman, J. P. Rousseau, J. N. Scheurer, B. Walton, and A. E. Dangor, "Electron acceleration by a wake field forced by an intense ultrashort laser pulse," Science **298**(5598), 1596–1600 (2002).
14. K. Nakajima, D. Fisher, T. Kawakubo, H. Nakanishi, A. Ogata, Y. Kato, Y. Kitagawa, R. Kodama, K. Mima, H. Shiraga, K. Suzuki, K. Yamakawa, T. Zhang, Y. Sakawa, T. Shoji, Y. Nishida, N. Yugami, M. Downer, and T. Tajima, "Observation of ultrahigh gradient electron acceleration by a self-modulated intense short laser pulse," Phys. Rev. Lett. **74**(22), 4428–4431 (1995).
15. C. A. Coverdale, C. B. Darrow, C. D. Decker, W. B. Mori, K. C. Tzeng, K. A. Marsh, C. E. Clayton, and C. Joshi, "Propagation of intense subpicosecond laser pulses through underdense plasmas," Phys. Rev. Lett. **74**(23), 4659–4662 (1995).
16. A. Modena, Z. Najmudin, A. E. Dangor, C. E. Clayton, K. A. Marsh, C. Joshi, V. Malka, C. B. Darrow, C. Danson, D. Neely, and F. N. Walsh, "Electron acceleration from the breaking of relativistic plasm waves," Nature **377**(6550), 606–608 (1995).
17. S. Masuda, E. Miura, K. Koyama, S. Kato, M. Adachi, T. Watanabe, K. Torii, and M. Tanimoto, "Energy scaling of monoenergetic electron beams generated by the laser-driven plasma based accelerator," Phys. Plasmas **14**(2), 023103 (2007).
18. K. Koyama, M. Adachi, E. Miura, S. Kato, S. Masuda, T. Watanabe, A. Ogata, and M. Tanimoto, "Monoenergetic electron beam generation from a laser-plasma accelerator," Laser Part. Beams **24**(01), 95–100 (2006).
19. Z. L. Chen, C. Unick, N. Vafaei-Najafabadi, Y. Y. Tsui, R. Fedosejevs, N. Naseri, P. E. Masson-Laborde, and W. Rozmus, "Quasi-monoenergetic electron beams generated from 7 TW laser pulses in N2 and He gas targets," Laser Part. Beams **26**(02), 147–155 (2008).
20. B. Hidding, K. U. Amthor, B. Liesfeld, H. Schwoerer, S. Karsch, M. Geissler, L. Veisz, K. Schmid, J. G. Gallacher, S. P. Jamison, D. Jaroszynski, G. Pretzler, and R. Sauerbrey, "Generation of quasimonoenergetic electron bunches with 80-fs laser pulses," Phys. Rev. Lett. **96**(10), 105004 (2006).
21. B. Hidding, M. Geissler, G. Pretzler, K. U. Amthor, H. Schwoerer, S. Karsch, L. Veisz, K. Schmid, and R. Sauerbrey, "Quasimonoenergetic electron acceleration in the self-modulated laser wakefield regime," Phys. Plasmas **16**(4), 043105 (2009).
22. E. Brunetti, R. P. Shanks, G. G. Manahan, M. R. Islam, B. Ersfeld, M. P. Anania, S. Cipiccia, R. C. Issac, G. Raj, G. Vieux, G. H. Welsh, S. M. Wiggins, and D. A. Jaroszynski, "Low emittance, high brilliance relativistic electron beams from a laser-plasma accelerator," Phys. Rev. Lett. **105**(21), 215007 (2010).
23. G. R. Plateau, C. G. R. Geddes, D. B. Thorn, M. Chen, C. Benedetti, E. Esarey, A. J. Gonsalves, N. H. Matlis, K. Nakamura, C. B. Schroeder, S. Shiraishi, T. Sokollik, J. van Tilborg, C. Toth, S. Trotsenko, T. S. Kim, M. Battaglia, T. Stöhlker, and W. P. Leemans, "Low-emittance electron bunches from a laser-plasma accelerator measured using Single-Shot X-Ray spectroscopy," Phys. Rev. Lett. **109**(6), 064802 (2012).
24. T. Hosokai, K. Kinoshita, T. Watanabe, K. Yoshii, T. Ueda, A. Zhidokov, M. Uesaka, K. Nakajima, M. Kando, and H. Kotaki, "Supersonic gas jet target for generation of relativistic electrons with 12 TW-50 fs laser pulse," presented at the Proc. EPAC, Paris,France, 3–7 Jun. 2002.
25. C. I. Moore, A. Ting, K. Krushelnick, E. Esarey, R. F. Hubbard, B. Hafizi, H. R. Burris, C. Manka, and P. Sprangle, "Electron trapping in self-modulated laser wakefields by Raman backscatter," Phys. Rev. Lett. **79**(20), 3909–3912 (1997).
26. Y. Ding, A. Brachmann, F. J. Decker, D. Dowell, P. Emma, J. Frisch, S. Gilevich, G. Hays, Ph. Hering, Z. Huang, R. Iverson, H. Loos, A. Miahnahri, H. D. Nuhn, D. Ratner, J. Turner, J. Welch, W. White, and J. Wu, "Measurements and simulations of ultralow emittance and ultrashort electron beams in the linac coherent light source," Phys. Rev. Lett. **102**(25), 254801 (2009).
27. J. P. Verboncoeur, A. B. Langdon, and N. T. Gladd, "An object-oriented electromagnetic PIC code," Comput. Phys. Commun. **87**(1-2), 199–211 (1995).
28. J. Schreiber, C. Bellei, S. P. D. Mangles, C. Kamperidis, S. Kneip, S. R. Nagel, C. A. J. Palmer, P. P. Rajeev, M. J. V. Streeter, and Z. Najmudin, "Complete temporal characterization of asymmetric pulse compression in a laser wakefield," Phys. Rev. Lett. **105**(23), 235003 (2010).

1. Introduction

One crucial requirement for realizing next-generation synchrotron light sources, colliders and linac-based free-electron lasers (FELs) is high brightness electron sources that possess extremely high-peak current and small normalized emittance. This is a tremendous challenge to traditional electron guns due to their relatively low accelerating gradient and strong bunch self-field interaction. Plasmas, however, can tolerate as high as 100 GV/m electric fields which is at least 3 orders of magnitude higher than radio-frequency (RF) cavities. Therefore laser plasma accelerators (LPA) can effectively damp the space charge instabilities and produce femtosecond electron bunches with micrometer size. After Tajima and Dawson first

#206679 - $15.00 USD Received 20 Feb 2014; revised 7 Apr 2014; accepted 14 Apr 2014; published 20 May 2014

proposed the laser wakefield accelerator (LWFA) [1], this research has witnessed tremendous progress, especially after the generation of quasi-monoenergetic electron beams [2–4]. Up to 3 GeV electron beams were reported by several teams [5–9]. One important mechanism responsible for generating well-collimated quasi-monoenergetic electron beams is so-called bubble/blowout acceleration, which requires ultra-short ($c\tau \sim \lambda_P$) and ultra-intense ($I > 10^{19}$ W/cm^2) laser pulses [10, 11]. It has been proved that the electron injection and acceleration process can be very stable under this mechanism which helps to reduce the beam geometric divergence angle. Another mechanism to generate quasi-monoenergetic electron bunches is self-modulated laser wakefield acceleration (SM-LWFA) which works with longer laser pulses and higher plasma densities [12–16]. It can produce a relatively small accelerating structure and provide large focusing forces, making it possible to further diminish the bunch size. Some recent experiments have demonstrated the probabilities of generating tens MeV quasi-monoenergetic electron beams by using several TW sub-hundred femtosecond laser pulses [17–21].

As one of the most important parameters in the conventional acceleration domain, the normalized emittance of the electron beam has been investigated by several groups in recent LPA experiments [22, 23]. It is defined as the volume occupied by the electron beam in the phase space times the electron energy and can be roughly estimated by $\varepsilon_{nx,ny} = \pi \cdot (\gamma \cdot \theta_{x,y}) \cdot \sigma_{x,y}$, where γ is the Lorenz factor, $\sigma_{x,y}$ and $\theta_{x,y}$ are the transverse rms beam size and the beam divergence angle, respectively. The product of γ and $\theta_{x,y}$ is called the normalized divergence angle (NDA) $\theta_{nx,ny}$. Since the beam size in LPA is relatively small, minimizing the NDA is crucial for the generation of ultralow emittance electron bunches. In the previous LPA experiments [2–9, 13–24], $\theta_{nx,ny}$ were hardly less than 500 mrad.

Here we present the generation of well-collimated quasi-monoenergetic electron bunches from a 2 TW, 80 fs, high-contrast laser facility. In contrast to the former LPA experiments using similar laser facilities, we chose a lower density to increase injection stabilities and effective acceleration length. By this simple method, a 23 ± 0.8 MeV quasi-monoenergetic electron beam with an ultra-small NDA of 92 mrad is produced, which is at least 5 times smaller than the previous published results.

2. Experimental setup

Our experiments were carried out on the XL-II Ti: sapphire laser facility at the Institute of Physics, Chinese Academy of Sciences. The 800 nm-wavelength p-polarized laser pulses are compressed to produce 80 fs, 160 mJ pulses on the target. The amplified spontaneous emission (ASE) contrast ratio was around 10^8 within the time scale of ten picoseconds. As shown in Fig. 1, the laser beam was focused by a gold-coated off-axis parabolic (OAP) mirror in an f/6 cone angle into a spot size of 8 μm at half maximum full width (FWHM), containing 35% of the laser power. The vacuum-focused laser intensities were 2.7×10^{18} W/cm^2, corresponding to the normalized vector potential $a_0 = 1.1$. The Rayleigh length Z_R is estimated to be 180 μm. The gas jet was generated by a pulsed slit-shaped (1.2 mm long and 10 mm wide) supersonic Laval nozzle [24]. The gas we used was helium.

#206679 - $15.00 USD Received 20 Feb 2014; revised 7 Apr 2014; accepted 14 Apr 2014; published 20 May 2014

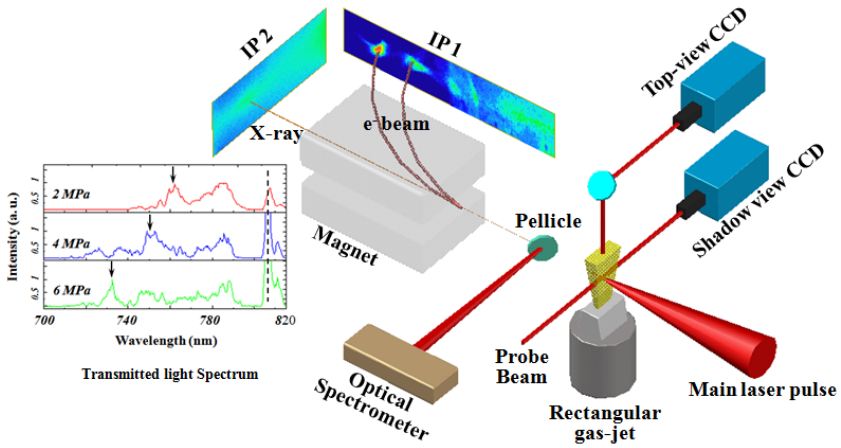

Fig. 1. Experimental setup: the figures near the Optical Spectrometer show the typical transmitted light spectrums at different backpressures. The dash line and the vertical arrows indicate the positions of the main laser (about 806 nm) and the positions of the anti-Stokes's peaks, respectively.

We used a spectrometer composed of a permanent dipole magnet (B_{max} ≈0.9 T) and two pieces of image plate (IP) with aluminum foils as laser light filters to detect the energy spectrum of the electron bunches. The two IPs were pasted on the side and exit of the magnet, allowing the measurement of the electrons from 3.5 MeV to 27 MeV (lateral) and 27 MeV to 175 MeV (forward), respectively. We could also obtain the beams' angular profiles on a phosphor screen placed on the exit window of the chamber by removing the magnet. A 16-bit Charge-Couple-Device (CCD) was used to record it. Another CCD camera with narrow band interference filters at 800 nm was placed perpendicular to both laser propagation and polarization directions (topview) to measure the length and position of the plasma channel. An 80 fs probe beam was employed to detect the shadow graph of the plasma. Additionally, transmitted light was reflected by a pellicle beam splitter with 98% transmission at 800 nm and collected by a fiber optic spectrometer from which the plasma density information can be acquired.

3. Results

In the current experiment, the ASE contrast was found to be a very important parameter for electron acceleration. No collimated electron bunches were observed if the contrast was lower than 10^6. On the other hand, when the contrast was higher than 10^7, well-collimated quasi-monoenergetic electron bunches were obtained after scanning the nozzle position and backpressure carefully. Obviously, high-contrast guarantees that the 2 TW laser pulse interacts with plasmas of pre-determined and fixed density as opposed to an evolving plasma density as in the case of low-contrast. Well self-focus is one of the necessary conditions for the generation of the quasi-monoenergetic beam. When quasi-monoenergetic electrons were generated, as shown in Figs. 2(a) and 2(b), long and narrow plasma channels were observed via topview and shadow view images. The laser beam propagates about 1 mm (~5 Rayleigh lengths) in the plasma without obvious diffraction. This indicates that the laser is well self-guided in the experiment which is consistent with the theoretical estimation: $P > P_c \approx 17 \times (n_c/n_e)$ GW ≈1.7 TW, provided the plasma density is $0.01n_c$, where P_c is the critical laser power for relativistic self-guiding in plasma, $n_c = m_e\omega^2/4\pi e^2$ is the critical density for propagation of the laser in the plasma, n_e is the plasma density, m_e and e are the electron rest mass and charge, respectively.

#206679 - $15.00 USD Received 20 Feb 2014; revised 7 Apr 2014; accepted 14 Apr 2014; published 20 May 2014

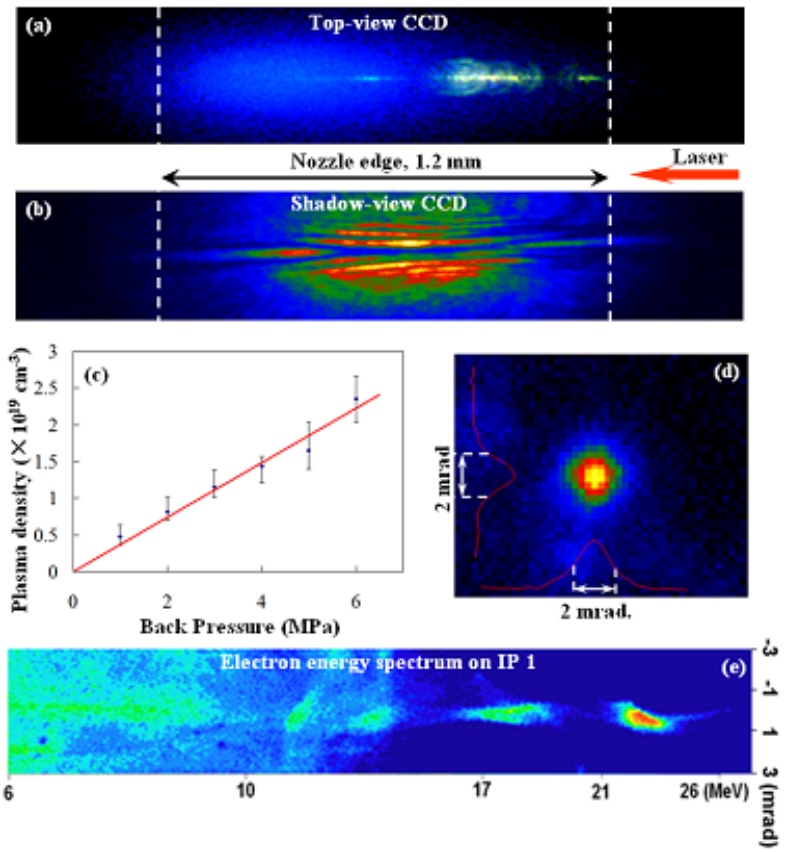

Fig. 2. Experiment results: typical top-view and shadow-view images are showed in (a) and (b), respectively. Pressure-dependent plasma densities are calculated from the corresponding transmitted light spectrum and presented in (c). Quasi-monoenergetic beams can only be generated in backing pressure between the red dashed lines in (c). Electron beam profile obtained on an 18 μm Al foil wrapped phosphor screen and spectra obtained after the dispersive magnet are shown in (d) and (e), respectively.

As shown in Fig. 1, a strong experimental confirmation of Raman Forward Scattering and self-modulation can be found in the transmitted light spectra [25]. The Stokes peak was not as clear as the anti-Stokes peak because the pellicle we used had a much higher reflectivity for high-frequency light ($\lambda \leq 780$ nm) than low-frequency light ($\lambda \geq 820$ nm). However, the plasma density can be calculated by taking: $\omega_p = \omega_0 \pm \Delta\omega$ and $n_e = m_e\omega_p^2/4\pi e^2$, where ω_p and ω_0 are electron plasma frequency and laser frequency, respectively. At relativistic intensities, the plasma frequency is reduced by a factor of $\gamma^{1/2}$, where $\gamma = (1 + a_0^2/2)^{1/2}$. As shown in Fig. 2(c), the plasma density varies from 4.8×10^{18} cm^{-3} to 2.8×10^{19} cm^{-3}, corresponding to the backpressure changing from 1 MPa to 6.5 MPa. When the pressure was lower than 4.5 MPa, no electron bunches could be observed in the experiments. When the backing pressure was higher than 5.5 MPa, electron bunches with extremely large divergence angles appeared. In these two cases, we didn't observe any electron bunches with the geometric divergence angles less than 15 mrad with >1000 shots. By comparison, well-collimated electron bunches with the divergence angle less than 5mrad could be generated stably when the pressure was between 4.5 and 5.5 MPa. Figure 3 shows the statistics of divergence angles of the consecutive 9 shots for the optimized pressure (5.0 MPa) and higher pressure (6.5 MPa), respectively. For P = 5.0 MPa, all the beams' divergence angles were less than 5 mrad, while for P = 6.5 MPa, the beam divergence angles were between 30 to 100 mrad. Comparing with Figs. 3(b) and 3(c), we can easily conclude that the injection and acceleration process is more

#206679 - $15.00 USD Received 20 Feb 2014; revised 7 Apr 2014; accepted 14 Apr 2014; published 20 May 2014

stable for the optimized pressure, which improves the electron beam's energy spread and transverse divergence angles. This implies that the injection and acceleration process is more stable in the optimized conditions with the plasma density between 1.6×10^{19}~2.1×10^{19} cm^{-3}.

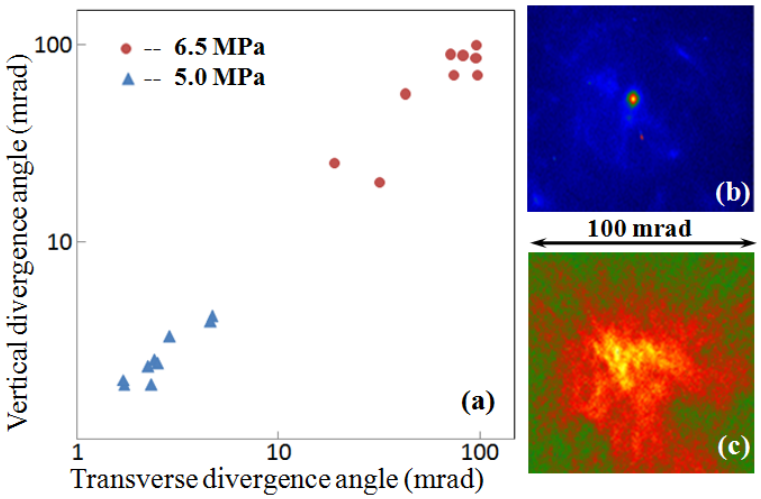

Fig. 3. (a) Electron beam divergence angles for the pressure equals 5.0 MPa (blue triangle) and 6.5 MPa, respectively. For each pressure, we select 9consecutive shots. Typical images for electron beam profile were presented for the pressure equals 5.0 MPa (b) and 6.5MPa (c), respectively.

A typical electron beam profile and energy spectrum are presented in Figs. 2(d) and 2(e). As shown in Fig. 2(d), the beam is intense and well-collimated. After calibration, the FWHM beam divergence $\theta_{x,\,y}$ = 2 mrad. From Fig. 2(e) we derive that the electron bunch is quasi-monoenergetic with an energy of 23 ± 0.8 MeV (about 7% in FWHM) and the bunch charge about 6 pC. The vertical beam divergence is also 2 mrad which agrees well with the beam profile measurement in Fig. 2(d). Hence, the transverse NDA in our experiment was about 92 mrad.

We compare our results to some previous reported LPA experiments and Table 1 presents the preliminary results:

Table 1. Comparison of NDA and Energy Spreads in Different LPA Experiments

Ref. #	Laser Power (TW)	$\theta_{x,\,y}$ (mrad)	γ	$\theta_{nx,\,ny} = \gamma \cdot \theta_{x,\,y}$ (mrad)	$\Delta E/E$
This work	2	2	46	92	± 3.5%
[2]	12.5	87	150	10350	± 3%
[3]	9	3	170	510	± 2%
[4]	30	10	340	3400	± 12%
[5]	40	2	2000	4000	± 2.5%
[7]	200	4	1600	6400	≥ ± 20%
[8]	1100	0.5	3600	1800	± 2.4%
[18]	2	40	14	560	≥ ± 15%
[20]	7.5	10	94	940	± 4.3%

As seen in Table 1, the NDA in our experiment is at least 5 times smaller than previous reports. If we assume $\sigma_{x,\,y}$ is about 2 μm as predicted in the following simulation, the normalized beam emittance is estimated to be less than 0.1π mm·mrad, which approaches or

#206679 - $15.00 USD Received 20 Feb 2014; revised 7 Apr 2014; accepted 14 Apr 2014; published 20 May 2014

even exceeds the most advanced electron guns' performance in the traditional accelerator domain [26].

4. Simulations and discussions

For further understanding of these experimental results, we carried out numerical simulations by using the 2-D PIC program OOPIC (Object Oriented Particle-in-Cell) [27]. In our simulations, the laser propagated along the x-direction with peak intensity $I_0 = 1 \times 10^{19}$W/cm^2, pulse duration $\tau = 80$ fs, wavelength $\lambda = 800$ nm and focal spot diameter $d_{FWHM} = 8$ μm. The simulation box was 100 μm in the x-direction and 60 μm in the y-direction and meshed into 2500 × 150 cells. Moving window technique was adopted and launched at the time of 0.95·Lx/c, where Lx is the length of the simulation box in x direction and c is the speed of light in vacuum, respectively. The total simulation length was 1 mm. We fixed the laser condition, scanned the plasma density and compared simulation and experimental results. Figure 4 reveals the evolution of the laser pulse and the resulting electron density distribution when the initial uniform plasma density is 1.74×10^{19} cm^{-3}.

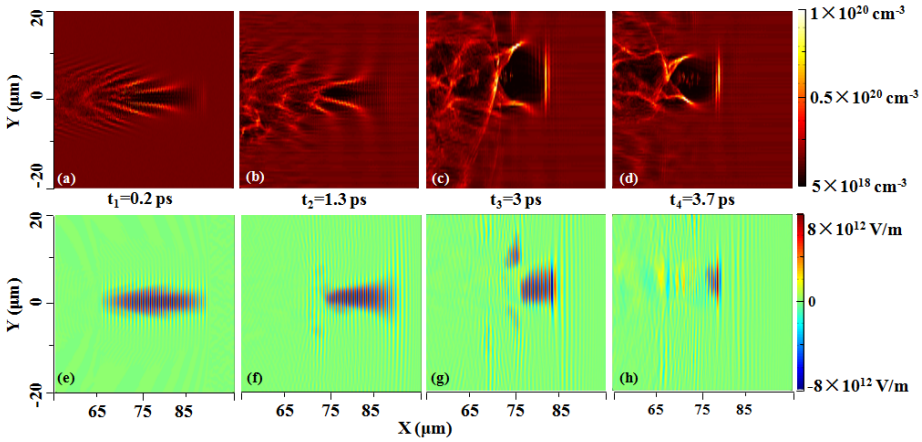

Fig. 4. Simulation results: 2D snapshots of plasma density (a-d) and laser pulse spatial evolution (e-h) at time $t_1 = 0.06$ mm/c (4(a) and 4(e)), $t_2 = 0.4$ mm/c (4(b) and 4(f)), $t_3 = 0.9$ mm/c (4(c) and 4(g)) and $t_4 = 1.1$ mm/c (4(d) and 4(h)).

At the beginning, as presented in Figs. 4(a), 4(b), 4(e) and 3(f), we see the laser pulse propagates in the plasma, the transverse ponderomotive force pushes the near-axis electrons away and produces a high-density electron sheath around and behind the laser pulse (Figs. 4(a) and 4(b)). At the same time, obvious self-focusing of the laser pulse is occurring (Figs. 4(e) and 4(f)).

Next, a transition from SM-LWFA to LWFA is observed in the simulation. Since the laser pulse length is longer than the plasma wavelength, the back flowing electrons encounter and couple with the latter part of the drive laser, leading to the erosion of the laser pulse tail. Another possible contribution to the rear pulse steepening is the variation of the group velocity across the laser pulse as discussed by Schreiber et al. [28]. As showed in Figs. 4(c) and 4(g) at 3 ps, the pulse duration has been reduced to about 30 fs while the longitudinal wakefields increased from 250 GV/m up to 600 GV/m. In such cases, a bubble-like electron-free cavity appears right behind the laser pulse. At this time, the pulse length is similar or even shorter than the nonlinear plasma wavelength. A group of background electrons are injected at the end of the bubble and are accelerated rapidly by the wakefields. Soon the head of the injected bunch (only a small part) catches up with the laser, aggravating the erosion and shortening the pulse length to about 5 μm within 1 ps (see Figs. 4(d) and 4(h)). Different from the higher density condition, the major part of the self-trapped electrons don't interact with the laser pulse. This is one of the most important reasons for producing well-collimated electron bunches. Meanwhile, the drive laser pulse is still strong enough to maintain a stable

#206679 - $15.00 USD Received 20 Feb 2014; revised 7 Apr 2014; accepted 14 Apr 2014; published 20 May 2014

accelerating structure for hundreds micrometers, ensuring most of the trapped electrons are accelerated to more than 20 MeV with a narrow energy spread before dephasing and depleting. The beam divergence angle could remain fairly small (~2 μm diameter) during acceleration because the transverse restoring forces were large and the interaction process was stable. This whole injection and acceleration process is like the standard LWFA, except the laser-plasma parameters' matching is spontaneous and much easier to realize in a real experiment. After density scanning in OOPIC, we found that the quasi-monoenergetic beams could only be generated in a narrow plasma density range (1.5~2.5 × 10^{19} cm^{-3}), which was similar to our experiment results. If operating at higher densities, the plasma wavelength is still much shorter than the modulated laser pulse when the self-injection happens. In addition, the self modulation and the hose instabilities destabilized the "bubble", hence no collimated and quasi-monoenergetic electron beams are generated, a phenomenon observed in former experiments [18–20]. When the plasma density was lower than 1.5 × 10^{19} cm^{-3}, the longitudinal wakefields couldn't increase to more than 500 GV/m due to weak self-focusing. As a result, there's hardly any background electrons self-trapped by the wakefields. In optimized conditions with the plasma density around 1.74 × 10^{19} cm^{-3}, we obtained a beam with a central energy of about 25 MeV and energy spread of 5% in simulation, as shown in Fig. 5, which was in good agreement with our experimental spectrum. The transverse NDA is about 85 mrad in the simulation, which also agrees well with the estimation based upon our experimental results.

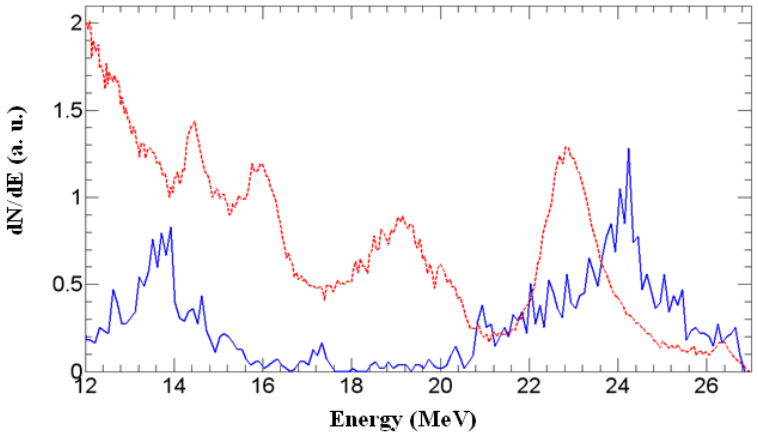

Fig. 5. Comparison of simulation (blue) and experimental (red dashed) electron energy spectra.

Based upon the simulation results, we can offer a simple physical explanation for the small normalized divergence angle bunches in our experiments:

As mentioned above, the normalized divergence angle is defined as $\theta_{nx,\,ny} = \gamma \cdot \theta_{x,\,y}$. For a self-injected electron in LPA, the longitudinal velocity is much larger than the transverse velocity and approximately equals the speed of light, so we can re-write the expression of $\theta_{nx,\,ny}$: $\theta_{nx,\,ny} = \gamma \cdot \theta_{x,\,y} = \gamma \cdot v_{x,\,y}/v_z \approx p_{x,\,y}/(m_e c)$, where $v_{x,\,y}$, v_z and $p_{x,\,y}$ are the transverse and longitudinal velocities of the electron and the electron's transverse momentum, respectively. So $\theta_{nx,\,ny}$ is found to be related only to the electron's transverse momentum. We can further divide $p_{x,\,y}$ into the initial transverse momentum before the self-injection $p^0_{x,\,y}$ and the momentum change during the injection and acceleration process $\delta p_{x,\,y}$, respectively.

For a blowout acceleration, the extremely high laser field increases $p^0_{x,\,y}$ and the relatively low transverse wakefield weakens the momentum damping. But owing to the shorter laser pulse length, the trapped electrons will experience stable injection and the acceleration continues until they catch up with the laser. This contrasts with a typical SM-LWFA, wherein the self-injected electrons are influenced by the laser's tail during the acceleration which leads to a significant increase of $\delta p_{x,\,y}$. As a result, the geometric divergence in SM-LWFA can

#206679 - $15.00 USD Received 20 Feb 2014; revised 7 Apr 2014; accepted 14 Apr 2014; published 20 May 2014

hardly be smaller than 10 mrad in the previous SM-LWFA experiments. For our case, we chose an optimum density to make a smooth transfer from SM-LWFA to LWFA. The small laser power guarantees a small $p^0_{x,y}$, while the stable injection and acceleration process leads to a small $\delta p_{x,y}$.

5. Summary

In summary, we present our recent LPA experimental results in which we obtained 23 MeV quasi-monoenergetic electron beams with small energy spread while using a laser with only 2 TW power interacting with He gas target. Despite the requirement of $\tau \cdot c > \omega_p$ and $P > P_c$, we emphasize the laser plasma parameters must be carefully scanned and matched to balance the SM-LWFA and LWFA regimes during the acceleration procedure. By taking advantage of the best features of SM-LWFA and LWFA, we succeed in reducing the initial transverse momentum and momentum change simultaneously, thereby producing a well-collimated electron beam with a normalized divergence angle as low as 92 mrad. The simulation results confirm the feasibility of this simple method. This new observation may build a new bridge between the conventional and novel acceleration communities and increase the applications for the LPA process.

Acknowledgments

We gratefully acknowledge to Dr. Y. Zheng and Dr. X. L. Ge for their helps on operating the XL-II laser facility. Author D. Z. Li also would like to thanks Dr. D. Wang and Dr. Y. Jiao in IHEP for fruitful discussions. This work was supported by the NSFC (Grant Nos. 11305185, 11175192, 60878014, 10974249, 10925421, 11105217, 11175119 and 11121504).